Experimental observation of water saturation effects on shear wave splitting in synthetic rock with fractures aligned at oblique angles

Kelvin Amalokwu[1,3], Mark Chapman[2,4], Angus I. Best[1], Jeremy Sothcott[1], Timothy A. Minshull[3] & Xiang-Yang Li[4].

[1]National Oceanography Centre, Southampton University of Southampton Waterfront Campus, European Way, Southampton SO14 3ZH United Kingdom

[2]University of Edinburgh School of Geosciences Grant Institute, the King's Building West Mains Road Edinburgh EH9 3JW, United Kingdom

[3]University of Southampton, National Oceanography Centre Southampton European Way Southampton SO14 3ZH United Kingdom

[4]Edinburgh Anisotropy Project British Geological Survey, Murchison House West Mains Road Edinburgh EH9 3LA, United Kingdom

Abstract

Fractured rocks are known to exhibit seismic anisotropy and shear wave splitting (SWS). SWS is commonly used for fractured rock characterisation and has been shown to be sensitive to fluid type. The presence of partial liquid/gas saturation is also known to affect the elastic properties of rocks. The combined effect of both fractures and partial liquid/gas saturation is still unknown. Using synthetic, silica-cemented sandstones with aligned penny-shaped voids, we conducted laboratory ultrasonic experiments to investigate the effect fractures aligned at an oblique angle to wave propagation would have on SWS under partial liquid/gas saturation conditions. The result for the fractured rock shows a saturation dependence which can be explained by combining a fractured rock model and a partial saturation model. At high to full water saturation values, shear wave splitting decreases as a result of the fluid bulk modulus effect on the quasi-shear wave. This bulk modulus effect is frequency dependent as a result of wave-induced fluid flow mechanisms, which would in turn lead to frequency dependent SWS. This result suggests the possible use of SWS for discriminating between full liquid saturation and partial liquid/gas saturation.

1. Introduction

Elastic wave propagation is strongly affected by the presence of partial liquid/gas saturation and by the presence of fractures. The combined effect of both is still poorly understood as little work has been done on saturation effects in fractured rocks. Aligned fractures are widespread in crustal rocks, causing seismic anisotropy (Crampin, 1981, Winterstein, 1992). The sensitivity of seismic waves to the presence of aligned fractures in the form of seismic anisotropy makes it possible to obtain fracture information from seismic data. A commonly used method is shear-wave splitting (SWS), given as the time delay between the fast and slow shear-waves, which is usually related to the fracture density (Crampin, 1985, Marson-Pidgeon and Savage, 1997, Liu *et al.*, 2003, Verdon and Kendall, 2011). This splitting results in two orthogonally polarized shear waves with velocities V_{s1} and V_{s2} for the pure shear and quasi-shear waves respectively. For isotropic rocks, Gassmann's formula predicts that the shear modulus of the rock is insensitive to saturation. However, in the anisotropic case fluid compressibility can affect shear wave propagation (Brown and Korringa, 1975), causing fluid-dependent shear wave splitting. This fluid-dependent shear wave splitting could be used as a diagnostic tool to infer the saturation properties of fractured reservoirs (e.g., Qian *et al.*, 2007).

Fluid-dependent shear wave splitting has been observed both in field data (Qian *et al.*, 2007, Van Der Kolk *et al.*, 2001) and laboratory experiments (Tillotson *et al.*, 2011). This fluid dependent SWS is indeed frequency dependent as shown by theoretical studies and field

studies (Marson-Pidgeon and Savage, 1997, Al-Harrasi *et al.*, 2011, Liu *et al.*, 2003, Chapman, 2003). Theoretical models are needed to interpret seismic data in terms of fracture properties and fluid properties. The combined effect of fluids (100% gas or liquid saturation) and aligned fractures have been studied theoretically and experimentally (e.g., Thomsen, 1995, Hudson, 1981, Hudson *et al.*, 2001, Chapman, 2003, Ass'ad *et al.*, 1992, Rathore *et al.*, 1995). The fluid independent relationship between fracture density and shear wave splitting for wave propagation at 90° to the fracture normal has been observed in laboratory experiments (e.g., Tillotson *et al.*, 2012, Rathore *et al.*, 1995) in line with theoretical predictions (e.g., Hudson, 1981). Theoretical predictions of fluid sensitivity of the slow shear-wave propagating at oblique angles to the fracture normal was observed in laboratory experiments by Tillotson *et al.* (2011) using a synthetic fractured sample cored at 45° to the fracture normal and saturated with single fluid phases of different viscosities. However, the seismic response to partial gas saturation in fractured rocks is still poorly understood at present, even though such conditions are commonly encountered in the Earth's crust.

Experimental investigation of water saturation effects have been limited to approximately isotropic rocks, most likely because of experimental limitations associated with fractured rock studies. A major limitation is that idealised fracture geometries (e.g., penny shaped cracks) often used in theoretical models as a mathematical approximation do not resemble natural fractures in rock, and it is difficult to control the introduction of aligned natural fractures in laboratory samples. Controlled fractured rock experiments have therefore required the use of synthetic rocks, leading to the use of synthetic materials to construct physical models, such as an epoxy matrix with embedded rubber discs to represent fractures (e.g., Ass'ad *et al.*, 1992, de Figueiredo *et al.*, 2013). These studies provided very useful results on elastic wave behaviour in fractured rocks, but they did not capture important wave-induced flow mechanisms (e.g., squirt flow; see Thomsen, 1995, Chapman, 2003). Recently,

Tillotson *et al.* (2012) produced novel synthetic silica cemented sandstones with controlled fracture geometry. These synthetic samples offer new possibilities for the validation and calibration of various aspects of theoretical models for fractured, porous rocks. In particular, the prediction of partial liquid/gas saturation effects is a complex problem; hence, we seek to guide the development of a suitable model through primary experimental observations.

Here, we present new laboratory experimental measurements of V_{s1} and V_{s2} as functions of water/air saturation in synthetic, silica-cemented sandstone containing fractures aligned at 45° to the fracture normal. The results show an interesting saturation dependence of SWS. We find that combining the corrected White (1975) model for partial saturation (sometimes referred to as the White and Dutta-Ode model – see Mavko *et al.* (2009)) with the fractured rock model of Chapman (2003) could give insight into the mechanisms controlling our experimental observations.

2. Methods

2.1. Synthetic Rock Samples

The samples used in this study (Figure 1a) were made by Tillotson (2012) as part of the same batch used by Tillotson *et al.* (2012), who give more details of the manufacturing process. The fractures are just visible on the surface of the sample in Figure 1a but Figure 1b shows the idealised distribution throughout the sample volume. The synthetic rock samples were made from a mixture of sand, kaolinite and aqueous sodium silicate gel using a similar approach to Rathore *et al.* (1995). A predetermined number of 2 mm diameter aluminium discs of 0.2 mm thickness were arranged on successive 4 mm layers of sand mixture. The blank sample (rock sample without fractures) was cored parallel to the layering and the fractured sample used in this study was cored at 45° to the fracture normal using a diamond drill bit. Each sample had a diameter of 50 mm and a length of 20-25 mm. Image analysis of

X-ray CT scans was used to obtain the fracture density, $\varepsilon_f = 0.0298 \pm 0.0077$, and the average fracture aspect ratio of 0.088 ± 0.001, for a sample cored at 90° to the fracture normal (that was not used in this study). As pointed out by Tillotson *et al.* (2012), this value includes voids created as a result of overlapping discs as well as discrete penny-shaped voids. Although the above fracture parameters were for a different sample to the one used in our experiments, both samples were made as part of the same batch, so are expected to have very similar fracture parameters.

The porosity and Klinkenberg corrected permeability were measured using Helium porosimetry and Nitrogen permeametry respectively. Permeability was measured in the direction of the core axis. The porosity and permeability are 30.43% and 40.7 mD for the blank sample, and 31.8% and 2.66 mD for the fractured sample, respectively. Note the difference in permeability between both samples, attributed to differences in grain packing during rock manufacturing stage and the direction in which the rocks were cored.
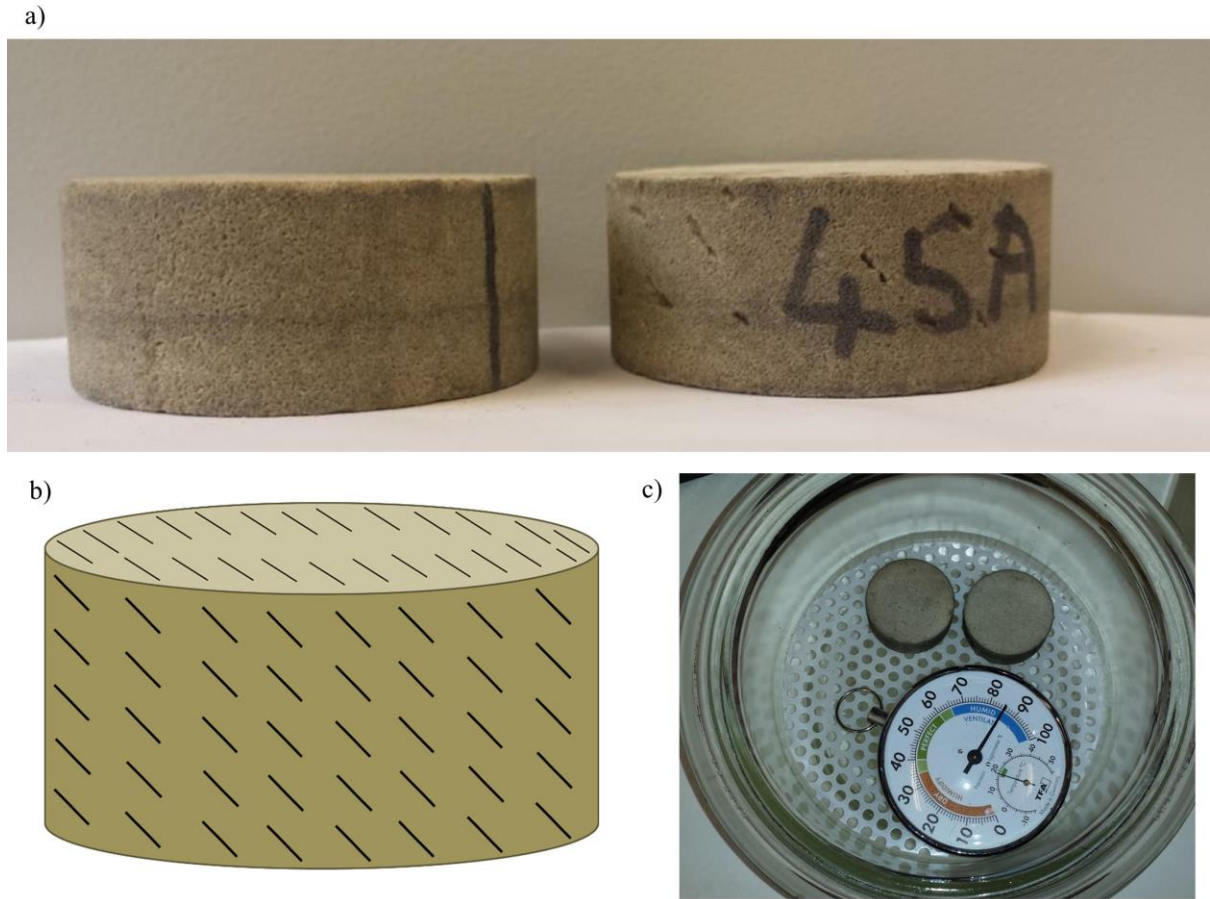
Figure 1. a) blank rock (left) and fractured rock (right). b) A schematic of the synthetic rock containing aligned fractures c) rock samples in vacuum desiccator containing saturated salt solution, and a hygrometer to verify the relative humidity.

2.2. Saturation methods

Partial saturation was achieved using the method described by Amalokwu *et al.* (2014). The rock samples were oven dried at 40°C for 48 hours and then placed under a vacuum until a pressure of 10^{-4} Pa was achieved, ensuring the rock was completely dry. Ultrasonic wave measurements were then taken on the dry samples. Partial water saturation (S_w) was achieved by placing the samples in an atmosphere of known and controlled relative humidity (RH) for between ten days to two weeks, until they had reached equilibrium. This method is known to give homogeneous S_w distributions for the lower S_w values (compared to

imbibition and drainage); similar methods have been used elsewhere (King *et al.*, 2000, Schmitt *et al.*, 1994, Papamichos *et al.*, 1997). Equilibration was monitored by weighing the samples at two-day intervals until the sample mass reached a constant value. The weighing scale used was an A&D GR-200-EC with accuracy up to 10^{-4} g; Sw can then be determined from rock porosity and dry weight. The temperature and relative humidity in the laboratory was controlled at 20°C and 55% respectively; as such, the samples were also weighed after the measurements to ensure no change in S_w had occurred as a result of exposure to a different RH atmosphere. There was hardly any loss of S_w, which was expected because of the much longer time for samples to absorb moisture and equilibrate compared to the relatively short time taken to make the ultrasonic measurements (< 2 hours in most cases). Also, measurements were not made with the sample directly exposed to the atmosphere as it was placed inside a high pressure rig (see McCann and Sothcott, 1992 for detailed equipment setup)

Controlled relative humidity (RH) was achieved using aqueous saturated salt solutions. Greenspan (1977) gave a range of salt solutions that would maintain a given RH at a particular temperature. The salts used and their approximate RH values (at $20\ ^{o}$C laboratory temperature) were Magnesium Nitrate (54%), Ammonium Sulphate (82%), Sodium Carbonate Decahydrate (92%), and Potassium Sulphate (98%) respectively, giving four different S_w values. A saturated aqueous salt solution was placed at the base of a vacuum desiccator, over which a wire gauze held the rocks in suspension (Figure 1c). A hygrometer was also placed on the wire gauze to monitor relative humidity. The desiccator was then placed under a vacuum for about two minutes and left to stand. This procedure was repeated whenever the rocks were taken out to be weighed. The maximum S_w achieved using this method was about 0.4 for the blank rock and 0.2 for the fractured rock.

The rocks were dried using the process described above, fully saturated in a vacuum with distilled, deionised and de-aired water and then pressurised to 7 MPa for at least 24 hours see (see McCann and Sothcott, 1992). Ultrasonic wave measurements were taken on the fully saturated samples. To achieve intermediate S_w values, we used a modified air/water drainage technique. In order to minimise effects of heterogeneous saturation distribution caused by drainage (Cadoret *et al.*, 1995, Knight *et al.*, 1998), the samples were wrapped in plastic ("cling") film after each drainage process. The wrapped samples were then placed in a desiccator containing the 98% RH solution, sealed (not vacuum sealed) and left for a minimum of 48 hours. The plastic film (and also the high RH atmosphere) prevents further air/water drainage, thus allowing capillary re-distribution over the length of time left to equilibrate ($\geq$ 48 hours). Although steps were taken to avoid/minimize heterogeneous saturation, it should be pointed out that the objective was to observe differences between the fractured rock and the blank rock response as a function of saturation using identical saturation and measurement methods.

2.3. Ultrasound Experiments

We measured ultrasonic wave velocity to an accuracy of $\pm$ 0.3% using the same pulse-echo (reflection) method as Tillotson *et al.* (2011) (see McCann and Sothcott, 1992 for detailed equipment description). Shear-wave splitting was measured by rotating the piezoelectric shear-wave transducer (while the sample was under elevated pressure) and observing the maximum and minimum signal amplitudes corresponding to S1 and S2 waves, respectively (see Best *et al.*, 2007).

The numerical modelling experiment of wave propagation in anisotropic media by Dellinger and Vernik (1994) showed that if the wavefront is propagating parallel or perpendicular to the layering (or in this case fractures), a true phase velocity is measured in

laboratory ultrasonic experiments. However, for wave propagation at 45$^\text{o}$ to the fracture normal, the wavefront can suffer a lateral translation dependent on the length of the sample and the strength of the anisotropy. If the lateral translation suffered by the wave is greater than the radius of the receiving transducer, then a group velocity is measured, not a phase velocity. Using equations (1) and (2) from Dellinger and Vernik (1994) to calculate the lateral translations, we get conservative estimates of 2 mm for the S1-waves and -0.16 mm for the S2-waves. We used estimates because measurements at other directions to the fracture normal are not available. We can conclude we measure phase velocity in our experimental setup as our transducer radius of 12.7 mm is much larger than the lateral translations suffered by the wavefronts. A similar conclusion was reached by Tillotson *et al.* (2011) using the same experimental setup as that used in this study.

Ultrasonic wave measurements were then taken at different partial saturation states of air/water, quantified by water saturation S_w.

3. Results

We present all results at an effective pressure of 40 MPa and a single frequency of 650 kHz obtained from Fourier analysis of broadband signals. Shear-wave splitting (SWS) is expressed as SWS (%) = 100 × (S1 − S2)/S1, where S1 and S2 are the parallel and perpendicular shear-wave velocities relative to the fracture direction, respectively. Figure 2 shows sample waveforms from the pulse-echo method; the waveforms are for dry and full water saturated cases for the fractured rock.
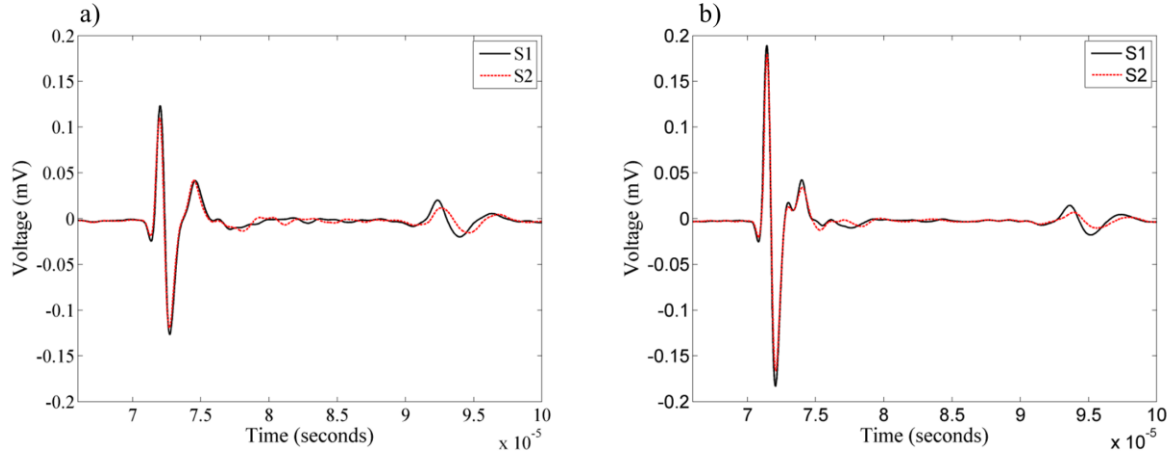
Figure 2. a) S1 and S2 waveforms for the dry fractured sample with S-wave propagation direction at 45˚ to the fracture normal. b) S1 and S2 waveforms for the water saturated fractured sample with S-wave propagation direction at 45˚ to the fracture normal. In both images, the first pulse is the reflection from the top of the rock while the second pulse is the reflection from the base of the rock.

In the blank sample, V_{s1} and V_{s2} have similar values for all S_w (Figure 3a), showing the shear-wave splitting induced by layering is negligibly small (~ 0.4 ± 0.6%) as shown in Figure 4a. The general trend of both shear velocities is a decrease with increasing water saturation, with the decline being more pronounced at intermediate S_w (between 0.2 − 0.7). For both shear waves, velocity is highest at $S_w = 0$ (dry) and lowest at $S_w = 1.0$ (full water saturation).
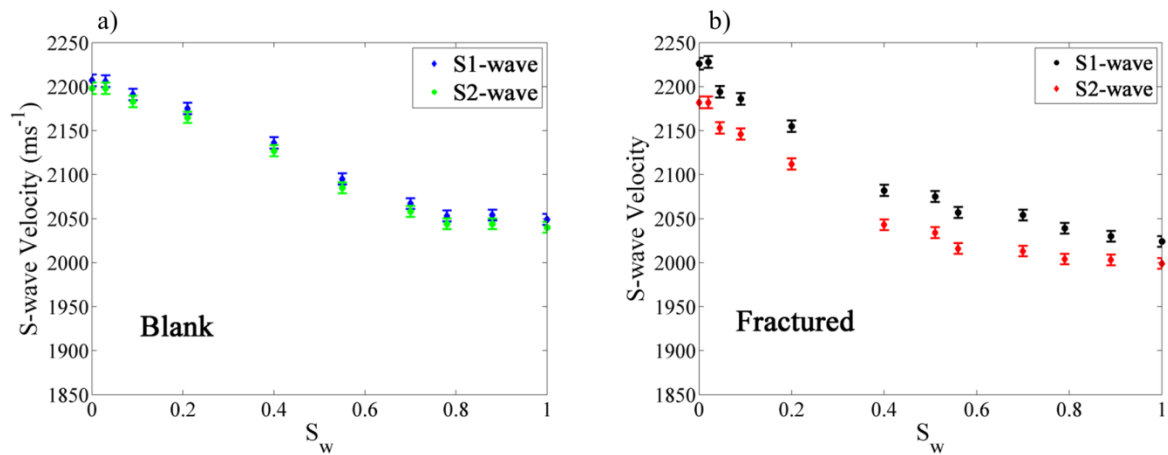
Figure 3. a) shows measured shear wave velocities versus S_w for the blank sample b) shows measured shear wave velocities versus S_w for the fractured sample.

In the fractured sample, there is significant shear wave splitting as expected (Figure 3b), the general trend of both shear-wave velocities is a decrease with increasing water saturation similar to the blank sample. Shear-wave splitting in the fractured rock (Figure 4b) begins at ~ $2 \pm 0.6\%$ at $S_w = 0$ (dry), remaining fairly constant until $S_w \approx 0.7$ followed by a steady decrease between $S_w \approx 0.8 - 1.0$, SWS being lowest at full water saturation.

Figures 4c and 4d show plots of the shear wave velocities at the different S_w values normalised by their individual dry velocities ($S_w = 0$). When both shear velocities are changing at the same rate, the data points overlap, however, in the fractured sample the S2-wave velocity appears to increase compared to the S1-wave velocity (Figure 4d), hence does not decrease at the same rate as the S1-wave velocity between $S_w \approx 0.8 - 1.0$. The SWS error bars show the minimum and maximum possible values of SWS. These were calculated from the maximum and minimum of velocity range based on absolute velocity errors of $\pm 0.3\%$.
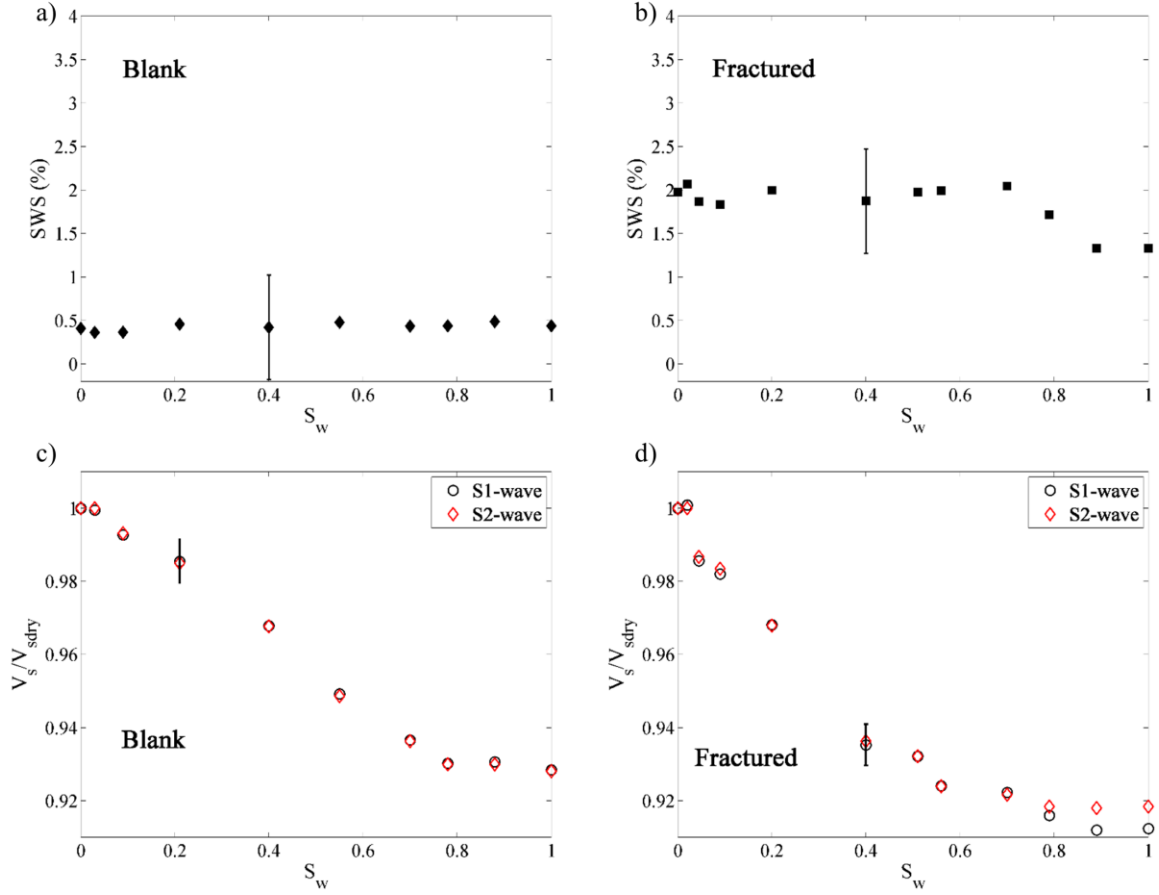
Figure 4. a) shows measured SWS versus S_w for the blank sample. b) shows measured SWS versus S_w for the fractured sample. c) shows ratios of the shear wave velocities to the dry shear wave velocity versus S_w for the blank sample. d) shows ratios of the shear wave velocities to the dry shear wave velocity versus S_w for the fractured sample. Error estimates are represented by the black vertical error bars.

4. Insight from modelling study and discussion

There is a lack of frequency dependent theoretical models for elastic wave velocities in partially saturated fractured rocks. Here, we combine two models to give some insight into the viscous mechanisms at play in our experiments. We combine the fractured rock model of Chapman (2003) (later modified by Chapman *et al.* (2003) to enable better practical

applicability) and the partial saturation model of White (1975). The stiffness tensor, C_{ijkl}, given by Chapman (2003) relating the contributions from the isotropic elastic tensor (C^0, with Lamé parameters, λ and μ), C^1 (pores), C^2 (microcracks) and C^3 (fractures) multiplied by the porosity (Φ_p), microcrack density (ε_c) and fracture density (ε_f) is of the form:

$$C_{ijkl} = C^o_{ijkl} - \Phi_p C^1_{ijkl} - \varepsilon_c C^2_{ijlk} - \varepsilon_f C^3_{ijkl} \tag{1}$$

This model is not designed for partial saturation, so in the expressions for the elastic tensor, we replace all terms apart from the fracture correction, with the Lamé parameters λ^o and μ^o obtained from the model of White (1975) for each water saturation value. The Lamé parameters λ^o and μ^o from White's model already contain pore corrections, and as shown by Chapman *et al.* (2003) ε_c can be set to zero in high porosity rocks which would make C^2 zero. We now have an equation of the form:

$$C_{ijkl} = C^{iso}_{ijkl}(\lambda^o, \mu^o) - \varepsilon_f C^3_{ijkl}; \tag{2}$$

where the term C^{iso}_{ijkl} is obtained from the Lamé parameters λ^o and μ^o calculated using the model of White (1975), after which the fracture correction C^3 from the model of Chapman *et al.* (2003) is applied. It should be pointed out here that the Lamé parameter, μ^o is the rock shear modulus which is assumed to be unaffected by saturation in White's model. Here the dispersion as a result of partial saturation is obtained from the model of White (1975) while anisotropy and dispersion at full water saturation are obtained from the model of Chapman (2003). The dispersion obtained from the model of Chapman (2003) is at full water saturation because the model was not developed for partial saturation. As we did not measure the full elastic tensor of the fractured rock, we only look to propose an explanation for our observations using a simple modelling exercise. It should be pointed out that since the fractured rock model of Chapman (2003) only predicts dispersion at full saturation, we

needed to include dispersion as a result of partial saturation. We do this by using White's model because it is a simple frequency-dependent saturation model. However, we do not restrict the cause of the dispersion in the partially saturated case to patchy saturation. White's model could be replaced with any other model that incorporates a frequency-dependent loss mechanism (e.g. viscous squirt flow).

Figure 5a shows White's model predictions of bulk modulus versus S_w at different frequencies. Figure 5b shows the corresponding predictions at 45° to the fracture normal after applying the fracture correction but without dispersion from the fractured rock model. This was achieved by setting the frequency in the model of Chapman (2003) to zero. The frequency dependence as a result of partial liquid/gas saturation can be seen. However, White's model is consistent with Gassmann's predictions at full water saturation because there are no saturati   on patches at full saturation and as such no dispersion is observed. As a result, the SWS at the different frequencies are the same at full water saturation (Figure 5b). These predictions were calculated using the blank rock properties as input into White's model and an arbitrary fractured rock fracture density, $\varepsilon_f = 0.023$ as input into the model of Chapman (2003). The gas patch size in White's model was kept constant (0.5 mm) and the frequency was varied, however, similar plots can be reproduced by varying the gas patch size and keeping the frequency constant. Setting the frequency in the model of Chapman (2003) to the same value as that used in White's model, the SWS becomes frequency dependent at full water saturation (Figure 5c). Figure 5d shows an enlarged portion of Figure 5c at higher S_w values to enable better visualisation of the results at different frequencies. It can be seen that the SWS versus S_w trend we observe can be reproduced qualitatively by applying a fracture correction to a partial saturation model. It then follows that if the S2 wave is sensitive to the bulk modulus of the saturating fluid, and the bulk modulus is frequency dependent, the SWS would also be frequency dependent.

We realise this is a rather simplistic approach of combining both models but our purpose here is simply to suggest an explanation for prediction of partial liquid/gas saturation effects. This is already a complex problem and the presence of fractures complicates it further. The actual mechanisms in an experiment like this, and their interactions would be very complex, however, using this simple approach we can at least gain some valuable insight into possible mechanisms causing the observed trend. The presence of partial gas saturation is known to cause dispersion believed to be as a result of wave induced fluid flow (e.g., mesoscopic and microscopic "squirt" flow) (see Müller *et al.*, 2010). White's model considers only one dispersion mechanism (mesoscopic flow) and this could lead to an under-prediction of the amount of dispersion as a result of partial saturation (e.g., Carcione *et al.*, 2003). An additional mechanism not considered by White's model, but believed to be responsible for the additional dispersion (at partial gas and full water saturation) observed at high frequencies, is squirt or local fluid flow (see Mavko and Nur, 1979, Winkler, 1985, Dvorkin *et al.*, 1994, Carcione *et al.*, 2003). The presence of fractures is also known to cause dispersion in saturated rocks through the squirt flow mechanism (see Chapman, 2003, Gurevich *et al.*, 2009). This squirt flow mechanism as a result of the presence of fractures is incorporated in the model of Chapman (2003). Although our modelling exercise only incorporates the squirt mechanism at full water saturation, using the simple modelling approach we adopted, it is straightforward to see that in the presence of squirt flow at partial liquid/gas saturation the fluid effect on the S2 wave would be even greater (increasing V_{s2} further), hence reducing the SWS. Dedicated partial saturation models could be introduced to make the modelling more rigorous in future (e.g., Kong *et al.*, 2013).

Although our observations are in the ultrasonic frequency range, it is reasonable to expect that these laboratory observations will be applicable to, or at least give guidance on, anisotropic saturation effects at the lower frequencies used in seismic field studies. Previous

ultrasonic experiments on synthetic fractured rocks already demonstrated the validity of frequency-dependent seismic anisotropy theory in response to different (fully saturated) fluid viscosities (Tillotson *et al.*, 2011, Tillotson, 2012). This implies that the geometric relationship between the meso-scale, penny-shaped fractures and the surrounding macro-porosity gives rise to viscous fluid flow losses that are representative of much lower frequencies through model scaling considerations (fracture size v. grain size v. wavelength). Hence, we would expect to observe representative wave-induced fluid flow losses associated with partial saturation effects, although there is no adequate model to describe these effects at present and thus make the link to seismic frequency behaviour. Although strictly speaking this experiment does not fall into the equivalent medium regime as the size of the fractures is comparable to the ultrasonic wavelength, we still observe important saturation dependence of SWS that we found could be explained using equivalent medium theory.
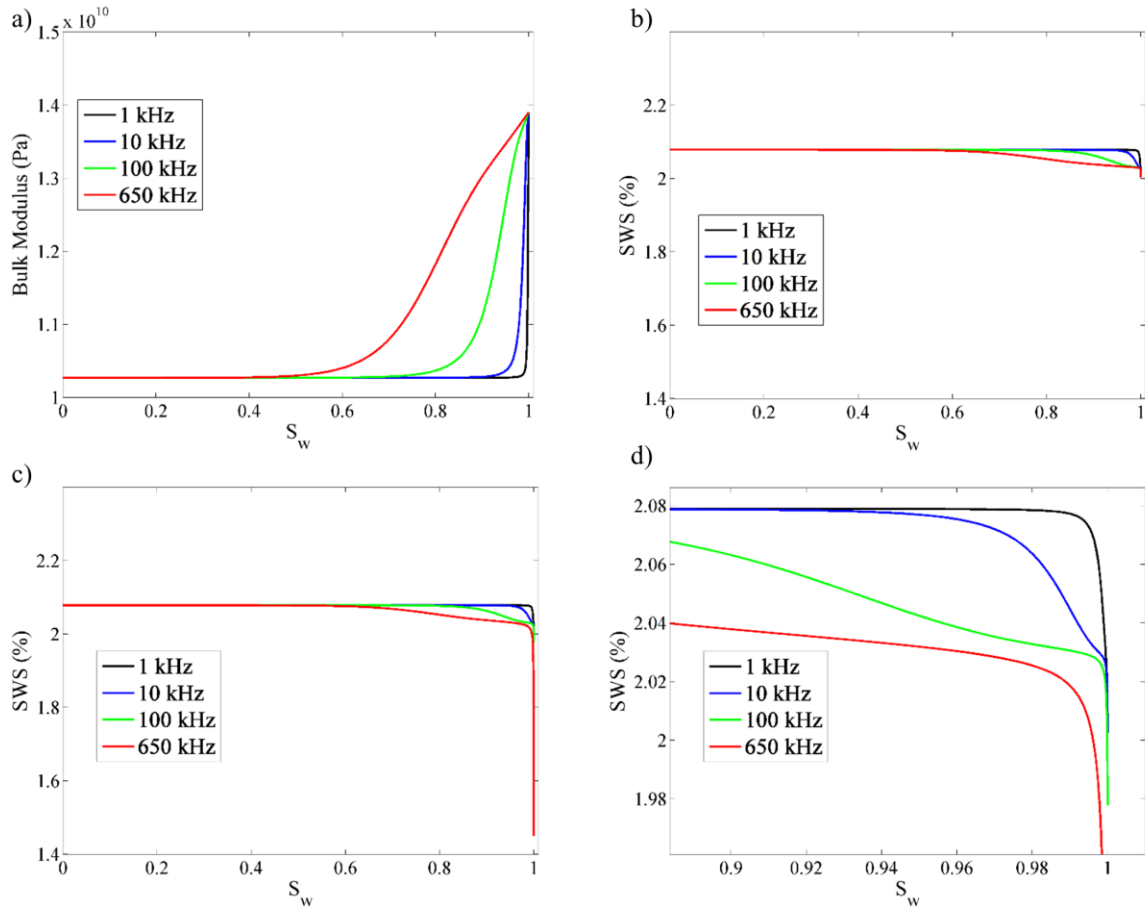
Figure 5. a) shows White's model predictions of bulk modulus versus S_w at different frequencies (using a constant patch size of 0.5 mm). b) shows SWS versus S_w obtained after applying fracture corrections to the bulk moduli obtained from Figure 5a. c) shows SWS versus S_w with squirt flow added to the results obtained in Figure 5b. d) shows an enlarged image of Figure 5c at higher S_w values to enable better visualisation of the model prediction at different frequencies. In Figures 5c and 5d, SWS at $S_w = 1$ for the different frequencies are 2.0, 2.0, 1.97 and 1.45 for 1, 10, 100 and 650 kHz respectively.

Our results show that SWS can be indicative of the presence of gas saturation in fractured reservoirs and could be useful in both exploration and production. The dispersion could also be exploited for gas saturation estimate. SWS information can be obtained from various types of seismic surveys such as passive monitoring of microseismicity, conventional seismic surveys, well logs, and vertical seismic profiles. These methods span different frequency ranges, which makes dispersion important. Knowledge of saturation effects on SWS could be important for the characterization of fractured reservoirs containing gas during exploration, production and monitoring. For example, it may give the ability to discriminate between gas and water saturated zones, as well as between less or more densely fractured zones. It may also be useful for the monitoring of reservoirs during gas injection such as for steam flooding, gas-driven reservoirs, injection of CO_2 for geological CO_2 storage and monitoring needed for climate change mitigation.

5. Conclusions

Novel synthetic sandstones containing aligned fractures were used to investigate the effect of liquid/gas saturation on SWS. The synthetic rock samples provide realistic analogues of naturally occurring sandstones. Within experimental errors, the results show

evidence for saturation dependent SWS in the rock with fractures aligned at 45° to the fracture normal. This is because in rocks with fractures aligned at oblique angles, the quasi-shear wave is sensitive to the bulk modulus of the saturating fluid, and hence to the effective bulk modulus of the rock-fluid mixture. This effective modulus is frequency dependent as a result of wave-induced fluid flow mechanisms which could be due to the presence of partial liquid/gas saturation, the presence of fractures or both. This acts to stiffen the rock leading to a higher effective bulk modulus, thus increasing the quasi-shear wave velocity and reducing the SWS, as the pure shear wave is not sensitive to the bulk modulus of the saturating fluid. By applying a fracture correction to a partial saturation model, we were able to explain our observations qualitatively. The results show that shear wave splitting in rocks with fractures aligned at oblique angles to wave propagation could potentially be used to distinguish between partial gas saturation and full liquid saturation.

Acknowledgements

References

Al-Harrasi, O.H., Kendall, J.M. & Chapman, M., 2011. Fracture characterization using frequency-dependent shear wave anisotropy analysis of microseismic data, *Geophysical Journal International,* 185**,** 1059-1070.

Amalokwu, K., Best, A.I., Sothcott, J., Chapman, M., Minshull, T. & Li, X.-Y., 2014. Water saturation effects on elastic wave attenuation in porous rocks with aligned fractures, *Geophysical Journal International*.

Ass'ad, J.M., Tatham, R.H. & McDonald, J.A., 1992. A physical model study of microcrack-induced anisotropy, *Geophysics,* 57**,** 1562-1570.

Best, A.I., Sothcott, J. & McCann, C., 2007. A laboratory study of seismic velocity and attenuation anisotropy in near-surface sedimentary rocks, *Geophysical Prospecting,* 55**,** 609-625.

Brown, R. & Korringa, J., 1975. On The Dependence Of The Elastic Properties Of A Porous Rock On The Compressibility Of The Pore Fluid, *GEOPHYSICS,* 40**,** 608-616.

Cadoret, T., Marion, D. & Zinszner, B., 1995. Influence of frequency and fluid distribution on elastic wave velocities in partially saturated limestones, *Journal of Geophysical Research: Solid Earth,* 100**,** 9789-9803.

Carcione, J., Helle, H. & Pham, N., 2003. White's model for wave propagation in partially saturated rocks: Comparison with poroelastic numerical experiments, *GEOPHYSICS,* 68**,** 1389-1398.

Chapman, M., 2003. Frequency-dependent anisotropy due to meso-scale fractures in the presence of equant porosity, *Geophysical Prospecting,* 51**,** 369-379.

Chapman, M., Maultzsch, S., Liu, E. & Li, X.-Y., 2003. The effect of fluid saturation in an anisotropic multi-scale equant porosity model, *Journal of Applied Geophysics,* 54**,** 191-202.

Crampin, S., 1981. A review of wave motion in anisotropic and cracked elastic-media, *Wave Motion,* 3**,** 343-391.

Crampin, S., 1985. Evaluation of anisotropy by shear‐wave splitting, *GEOPHYSICS,* 50**,** 142-152.

de Figueiredo, J.J.S., Schleicher, J., Stewart, R.R., Dayur, N., Omoboya, B., Wiley, R. & William, A., 2013. Shear wave anisotropy from aligned inclusions: ultrasonic frequency dependence of velocity and attenuation, *Geophysical Journal International*.

Dellinger, J. & Vernik, L., 1994. Do traveltimes in pulse-transmission experiments yield anisotropic group or phase velocities?, *Geophysics,* 59**,** 1774-1779.

Dvorkin, J., Nolen-Hoeksema, R.C. & Nur, A., 1994. The squirt-flow mechanism; macroscopic description, *Geophysics,* 59**,** 428-438.

Greenspan, L., 1977. Humidity Fixed Points of Binary Saturated Aqueous Solutions, *J. Res. Nat. Bur. Stand. (U.S.) - A (Phys. And Chem.),* 81A**,** 89-96.

Gurevich, B., Brajanovski, M., Galvin, R.J., Müller, T.M. & Toms-Stewart, J., 2009. P-wave dispersion and attenuation in fractured and porous reservoirs – poroelasticity approach, *Geophysical Prospecting,* 57**,** 225-237.

Hudson, J.A., 1981. Wave speeds and attenuation of elastic waves in material containing cracks, *Geophysical Journal of the Royal Astronomical Society,* 64**,** 133-150.

Hudson, J.A., Pointer, T. & Liu, E., 2001. Effective-medium theories for fluid-saturated materials with aligned cracks, *Geophysical Prospecting,* 49**,** 509-522.

King, M.S., Marsden, J.R. & Dennis, J.W., 2000. Biot dispersion for P- and S-wave velocities in partially and fully saturated sandstones, *Geophysical Prospecting,* 48**,** 1075-1089.

Knight, R., Dvorkin, J. & Nur, A., 1998. Acoustic signatures of partial saturation, *GEOPHYSICS,* 63**,** 132-138.

Kong, L., Gurevich, B., Müller, T.M., Wang, Y. & Yang, H., 2013. Effect of fracture fill on seismic attenuation and dispersion in fractured porous rocks, *Geophysical Journal International,* 195**,** 1679-1688.

Liu, E., Queen, J.H., Li, X.Y., Chapman, M., Maultzsch, S., Lynn, H.B. & Chesnokov, E.M., 2003. Observation and analysis of frequency-dependent anisotropy from a multicomponent VSP at Bluebell-Altamont field, Utah, *Journal of Applied Geophysics,* 54**,** 319-333.

Marson-Pidgeon, K. & Savage, M.K., 1997. Frequency-dependent anisotropy in Wellington, New Zealand, *Geophysical Research Letters,* 24**,** 3297-3300.

Mavko, G., Mukerji, T. & Dvorkin, J., 2009. *The Rock Physics Handbook,* edn, Vol., pp. Pages, Cambridge University Press.

Mavko, G.M. & Nur, A., 1979. Wave attenuation in partially saturated rocks, *Geophysics,* 44.

McCann, C. & Sothcott, J., 1992. Laboratory measurements of the seismic properties of sedimentary rocks, *Geological Society, London, Special Publications,* 65**,** 285-297.

Müller, T., Gurevich, B. & Lebedev, M., 2010. Seismic wave attenuation and dispersion resulting from wave-induced flow in porous rocks — A review, *GEOPHYSICS,* 75**,** 75A147-175A164.

Papamichos, E., Brignoli, M. & Santarelli, F.J., 1997. An experimental and theoretical study of a partially saturated collapsible rock, *Mechanics of Cohesive-frictional Materials,* 2**,** 251-278.

Qian, Z., Chapman, M., Li, X., Dai, H., Liu, E., Zhang, Y. & Wang, Y., 2007. Use of multicomponent seismic data for oil-water discrimination in fractured reservoirs, *The Leading Edge,* 26**,** 1176-1184.

Rathore, J.S., Fjaer, E., Holt, R.M. & Renlie, L., 1995. P- and S-wave anisotropy of a synthetic sandstone with controlled crack geometryl1, *Geophysical Prospecting,* 43**,** 711-728.

Schmitt, L., Forsans, T. & Santarelli, F.J., 1994. Shale testing and capillary phenomena, *Int. J. Rock Mech. Min. Sci. & Geomech. Abstr.,* 31**,** 411 – 427.

Thomsen, L., 1995. Elastic anisotropy due to aligned cracks in porous rock, *Geophysical Prospecting* 43**,** 805-829.

Tillotson, P., Chapman, M., Best, A.I., Sothcott, J., McCann, C., Shangxu, W. & Li, X.-Y., 2011. Observations of fluid-dependent shear-wave splitting in synthetic porous rocks with aligned penny-shaped fractures‡, *Geophysical Prospecting,* 59**,** 111-119.

Tillotson, P., Sothcott, J., Best, A.I., Chapman, M. & Li, X.-Y., 2012. Experimental verification of the fracture density and shear-wave splitting relationship using synthetic silica cemented sandstones with a controlled fracture geometry, *Geophysical Prospecting,* 60**,** 516-525.

Tillotson, P.R., 2012. A laboratory investigation of frequency-dependent seismic anisotropy in fractured rocks, Ph.D. thesis, University of Southampton, Southampton.

Van Der Kolk, C.M., Guest, W.S. & Potters, J.H.H.M., 2001. The 3D shear experiment over the Natih field in Oman: the effect of fracture-filling fluids on shear propagation, *Geophysical Prospecting,* 49**,** 179-197.

Verdon, J.P. & Kendall, J.M., 2011. Detection of multiple fracture sets using observations of shear-wave splitting in microseismic data, *Geophysical Prospecting,* 59**,** 593-608.

White, J.E., 1975. Computed seismic speeds and attenuation in rocks with partial gas saturation, *Geophysics,* 40**,** 224-232.

Winkler, K., 1985. Dispersion analysis of velocity and attenuation in Bera Sandstone, *Journal of Geophysical Research,* 90**,** 6793-6800.

Winterstein, D., 1992. How shear-wave properties relate to rock fractures; simple cases, *The Leading Edge,* 11**,** 21-28.